arXiv:cond-mat/0308251v2 [cond-mat.stat-mech] 27 Nov 2004

Local graph alignment and motif search in biological networks

Johannes Berg and Michael Lässig
Institut für Theoretische Physik, Universität zu Köln,
Zülpicherstr. 77, 50937 Köln, Germany

January 2, 2022

PNAS, **101** (41) 14689-14694 (2004),

Interaction networks are of central importance in post-genomic molecular biology, with increasing amounts of data becoming available by high-throughput methods. Examples are gene regulatory networks or protein interaction maps. The main challenge in the analysis of these data is to read off biological functions from the topology of the network. Topological *motifs*, i.e., patterns occurring repeatedly at different positions in the network have recently been identified as basic modules of molecular information processing. In this paper, we discuss motifs derived from families of mutually similar but not necessarily identical patterns. We establish a statistical model for the occurrence of such motifs, from which we derive a scoring function for their statistical significance. Based on this scoring function, we develop a search algorithm for topological motifs called *graph alignment*, a procedure with some analogies to sequence alignment. The algorithm is applied to the gene regulation network of *E. coli*.

The vast amount of sequence data collected over the past two decades is at the heart of quantitative molecular biology. Biological information is extracted from these data mainly by analyzing similarities between sequences. This approach is based on efficient *sequence alignment* algorithms and a statistical theory to assess the significance of the results (see [1]). Its ultimate goal is to infer functional relationships from correlations between sequences. Over the last few years, however, it has become clear that functions in many cases cannot be identified at the level of single genes. A given function may require the cooperative action of several genes, and conversely, a given gene may play a role in quite different functional contexts. The genome is thus a highly interactive system and the expression of a gene depends on the activity of other genes. The pathways of these interactions are encoded in so-called *regulatory networks*. Similarly complex networks govern *signal transduction*, that is, the influence of external signals on gene expression, or *protein interactions*, that is, the ability of two or more proteins to form a bound state in a living cell.

A few exemplary cases of gene networks have been studied in much detail, such as the regulation of early development in the sea urchin *Strongylocentrotus purpuratus* [2] or in *Drosophila* [3]. In some approximation, these structures can be understood as *logical networks*: the expression level of a gene is reduced to a binary variable (*on* or *off*) and is specified in terms of binary input data, i.e., the expression levels of its "upstream" genes.

On the other hand, a large amount of data on molecular interaction networks is now obtained by high-throughput experiments, for example protein interaction maps in yeast [4] or gene expression arrays [5]. In these arrays, one probes the activity of an entire genome, rather than of just a few genes. However, the detailed logical connection of interaction pathways is typically lost. The information is reduced to a *topological network*, that is, a set of nodes (representing, e.g., genes or proteins) and links representing their pairwise interactions. These links can be *directed* as in the case of regulatory interactions or *undirected* as for protein-protein binding. The amount of topological data on molecular networks is expected to increase rapidly in the next few years, paralleling the earlier explosion of sequence data.

What can be learned from these data? Using the network topology alone, can we distinguish patterns of biological function from random background? The purpose of this paper is to develop a "bioinformatics" approach to the search for local modules in networks. We discuss a heuristic *search algorithm* and its statistical grounding in a stochastic model of *network evolution*. This approach is designed to complement experiments in specific organisms by large-scale

database searches.

In two seminal studies [6, 7], it has recently been shown that topological networks indeed contain statistically significant patterns indicative of biological functions. These *motifs* are patterns which occur more frequently in the observed network than expected in a suitable null ensemble. The motifs found so far have been identified because they occur *identically* at different positions in a network.

If network evolution is a stochastic process, however, functionally related motifs do not need to be topologically identical. Hence, the notion of a motif has to be generalized to a stochastic one as well. Variations arise due to uncertainties in the network data, or – more importantly – because some of the interactions can change without affecting the functionality of the motif. This "noise" is an important characteristic of biological systems, familiar from sequence analysis where one searches for local sequence similarities blurred by mutations and insertions/deletions, rather than for identical subsequences. It leads us to the notion of a *probabilistic motif* where each link occurs with a certain likelihood. Probabilistic motifs arise as consensus from finding a family of "sufficiently" similar subgraphs in a network. The search for mutually similar subgraphs and their probabilistic motifs is the central issue of this paper.

The motifs of interest here are non-random in two ways: they have an enhanced number of internal links, associated e.g. with feedback, and they appear in a significant number of subgraphs. Identifying these *local* deviations from randomness in networks requires a statistical theory of local graph structure, which we establish in this paper. This is a complementary approach to the global statistics measured by the connectivity distribution [8] or connectivity correlations [9, 10] of a network.

Our approach leads to an algorithmic procedure termed *local graph alignment*, which is conceptually similar to sequence alignment. It is based on a *scoring function* measuring the statistical significance for families of mutually similar subgraphs. This scoring involves quantifying the significance of the individual subgraphs as well as their mutual similarity, and is thus considerably more complicated than for families of identical motifs. Our scoring function is derived from a stochastic model for network evolution. There is indeed evidence that network evolution can be described as a stochastic process. For example, the comparison of the regulatory networks for early development in several *Drosophila* species has revealed the continuous buildup and loss of gene interactions following an approximate molecular clock [11]. Yet little is known about the specific pathways of network evolution. Our scoring function is compatible with divergent evolution of subgraphs but also with convergent evolution towards a common functional motif. These pathways can be illustrated by a comparison with sequence evolution. An example of convergent evolution is the formation of sequence motifs serving as binding sites of specific enzymes [12, 13]. An example of divergent evolution is a set of sequences stemming from a common ancestor undergoing mutations independently. The probabilistic grounding of graph alignment allows us to infer optimal scoring parameters by a maximum-likelihood procedure [14].

As a computational problem, graph alignment is more challenging than sequence alignment. Sequences can be aligned in polynomial time using dynamic programming algorithms. For graph alignment, a polynomial-time algorithm probably does not exist. Already simpler graph matching problems such as the *subgraph isomorphism problem* (deciding whether a graph contains a given subgraph) [15, 16] or finding the *largest common subgraph* of two graphs [17] are NP-complete and NP-hard, respectively. Thus, an important issue for graph alignment is the construction of efficient heuristic search algorithms. Here we solve this problem by mapping graph alignment onto a spin model familiar in statistical physics, which can be treated by simulated annealing.

This paper is structured as follows. In the first part, we discuss the statistics of local subgraphs based on a probabilistic model. This is done in three steps: (i) an individual subgraph with an enhanced number of internal links, (ii) a subgraph in the presence of a template motif specifying the functional importance of each link, and (iii) correlated subgraphs, whose common pattern is to be inferred from the data instead of being given as a template. We then construct a scoring function designed to distinguish sets of statistically significant network motifs with an enhanced number of links from a background of other patterns. High-scoring motifs are found by an alignment algorithm, details of which are described in the supporting text. In the second part of the paper, we apply this method to the regulatory network of *Escherichia coli* and discuss the probabilistic motifs found. The statistics of these motifs is used to test the assumptions of our probabilistic model.

Graphs and patterns

A topological network or *graph* is a set of *nodes* and *links*. Labeling the nodes by an index $r = 1, \ldots, N$,

the network is described by the *adjacency matrix* $\mathbf{C}$, which has entries $C_{rr'} = 1$ if there is a directed link from node r to node r' and $C_{rr'} = 0$ otherwise. Graphs with a generic adjacency matrix are called *directed*. The special case of a symmetric adjacency matrix can be used to describe *undirected* graphs. The *in* and *out connectivities* of a node, $k_r^+ = \sum_{r'} C_{r'r}$ and $k_r^- = \sum_{r'} C_{rr'}$, are defined as the number of in- and outgoing links, respectively. The total number of links is denoted by $K = \sum_{r,r'} C_{rr'}$. The networks considered here are *sparse*, i.e., their average connectivity K/N is of order 1.

A *subgraph* G is given by a subset of n vertices $\{r_1, \dots r_n\}$ and the resulting restriction of the adjacency matrix. More precisely, we define the matrix $\mathbf{c}(G, \mathcal{A})$ with the entries $c_{ij} = C_{r_i r_j}$ $(i, j = 1, \dots, n)$ specifying the internal links of the subgraph for a given order $\mathcal{A}$ of the nodes. This matrix $\mathbf{c}$ is called a *pattern*, which is contained in the subgraph. The definition of a pattern used here implies that two patterns are counted as separate if the matrices $\mathbf{c}$ and $\mathbf{c}'$ are different. This assumes that nodes are distinguishable by their biochemical identity and their functional role even if they are at symmetric positions, i.e., if $\mathbf{c}$ and $\mathbf{c}'$ differ only by the labeling of the nodes. An alternative definition would count two matrices $\mathbf{c}$ and $\mathbf{c}'$ related by a relabeling as defining an identical pattern. Which definition is more appropriate depends on the particular biological application.

The most important characteristic of patterns for what follows is their number of internal links,

$$L(\mathbf{c}) = \sum_{i,j} c_{ij}. \tag{1}$$

Fig. 1 shows two subgraphs that differ in the values of L.

Graph alignments and motifs

A *graph alignment* is defined by a set of several subgraphs G^α $(\alpha = 1, \dots, p)$ and a specific order of the nodes $\{r_1^\alpha, \dots, r_n^\alpha\}$ in each subgraph; this joint order is again denoted by $\mathcal{A}$. For simplicity, we assume here that the subgraphs are of the same size n, but it is not difficult to generalize our approach in order to include subgraphs of different size. For a given set of p mutually disjoint subgraphs, there are $(n!)^p$ different alignments. An alignment associates each node in a subgraph with exactly one node in each of the other subgraphs. This can be visualized by n "strings", each connecting the p nodes with the same index i as shown in fig. 1 (c).

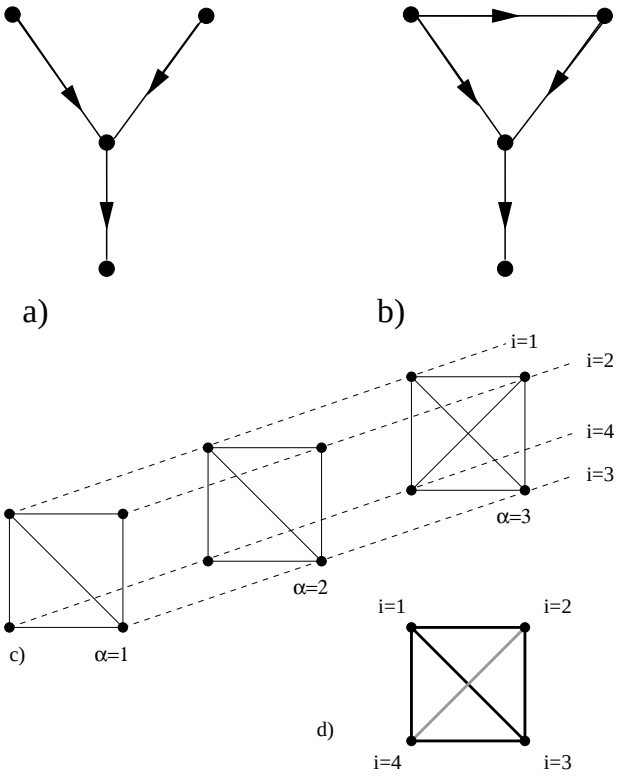


Figure 1: **Motifs and alignment in topological networks.** (a) A randomly chosen connected subgraph is likely to be a tree, i.e., it has a the number of internal links links equal to its number of nodes minus 1. (b) Putatively functional subgraphs are distinguished by internal loops, i.e., by a higher number of internal links. (c) An alignment of three subgraphs with four nodes each. Each nodes carries an index $\alpha = 1, 2, 3$ labeling its subgraph and an index $i = 1, 2, 3, 4$ given by the order of nodes within the subgraph. Nodes with the same index i are joined by dashed lines, defining a one-to-one mapping between any two subgraphs. Network links are shown as solid lines (with their arrows suppressed for clarity). (d) The consensus pattern of this alignment. Each link occurs with a likelihood $\bar{c}_{ij}$ indicated by the gray scale.

A given alignment $\mathcal{A}$ specifies a pattern in each subgraph, we write $\mathbf{c}^\alpha \equiv \mathbf{c}(G^\alpha, \mathcal{A})$. The *consensus pattern* of this alignment is given by the matrix

$$\overline{\mathbf{c}} = \frac{1}{p} \sum_{\alpha=1}^{p} \mathbf{c}^\alpha. \tag{2}$$

This is a *probabilistic pattern*, the entry $\overline{c}_{ij}$ denoting the likelihood that a given link is present in the aligned subgraphs. For any two aligned subgraphs

G^α and G^β, we can define the *pairwise mismatch*

$$M(\mathbf{c}^\alpha, \mathbf{c}^\beta) = \sum_{i,j=1}^{n} [c_{ij}^\alpha (1 - c_{ij}^\beta) + (1 - c_{ij}^\alpha) c_{ij}^\beta] \ . \quad (3)$$

The mismatch is 0 if and only if the matrices $\mathbf{c}^\alpha$ and $\mathbf{c}^\beta$ are equal, and is positive otherwise. It can be considered as a Hamming distance for aligned subgraphs. The average mismatch over all pairs of aligned subgraphs, $\overline{M} \equiv M(\overline{\mathbf{c}}, \overline{\mathbf{c}})$, is termed the *fuzziness* of the consensus pattern $\overline{\mathbf{c}}$. Analogously, the average number of internal links is denoted by $\overline{L} \equiv L(\overline{\mathbf{c}})$.

We now define *network motifs* as statistically significant consensus patterns of graph alignments, which are distinguished by a high number of internal links and low fuzziness. Clearly, this definition is mathematically loose before we quantify the statistical significance. This will be done in the next three sections.

Guided by the results of refs. [6, 7], we take an enhanced number of internal links as a topological indicator of possible functional modules in networks. The additional links beyond a treelike topology can be associated with feedback or feed-forward loops in transcription networks, or clusters in protein interaction networks. For example, the triangle shown in fig. 1 (b) can be interpreted [6] as a low-frequency bandpass filter: the central node is activated if both top nodes are active. However, the right hand node is activated by that on the left with a small delay, so the central node is activated provided the left node is active for a time *longer* than this delay. The non-treelike nature of this motif is crucial for its function. On the other hand, most randomly chosen *connected* subgraphs would be treelike. Clearly, an enhanced number of internal links is but the simplest topological indicator of putative functionality, and more detailed ways of identifying network motifs are likely to emerge in the future.

Statistics of individual subgraphs

In order to quantify the statistical significance of a given number of internal links, we first compute the relevant probability distribution in a suitable random graph ensemble, which is generated by an unbiased sum over all graphs with the same number of nodes and the same connectivities k_r^-, k_r^+ $(r = 1, \ldots, N)$ as in the data set but randomly chosen links [18, 10]. This *null ensemble* is appropriate for biological networks, whose connectivity distribution generally differs markedly from that of a random graph with uniformly distributed links. In the null ensemble, the probability of finding a directed link from node r_i to node r_j is in good approximation given by $w_{ij} = k_{r_i}^- k_{r_j}^+ / K$ [19]. Hence, a given subset of nodes $\{r_1, \ldots, r_n\}$ forms a subgraph G with probability

$$P_0(G) = \prod_{i,j=1}^{n} (1 - w_{ij})^{1 - c_{ij}} w_{ij}^{c_{ij}} . \quad (4)$$

This expression neglects double links, which can be included as in [19]. The probability $P_0(G)$ depends on the pattern $\mathbf{c}(G)$ of the subgraph, as well as on its environment given by the connectivities k_i^+, k_i^- $(i = 1, \ldots, n)$. In this ensemble, the expected number of internal links per node is small, $\langle L \rangle_0 / n \sim n/N$, where we denote the average over a given ensemble by $\langle\rangle$. Hence, most random subgraphs in a large and sparse graph are disconnected. Within the subset of connected subgraphs, most are treelike. (Later we will be interested in the subset of non-treelike subgraphs, and this will require a modification of the null ensemble.)

We now assume that subgraphs containing network motifs are generated by a different ensemble $P_\sigma(G)$. The probability that a given pair of nodes carries a link is enhanced by a factor e^σ relative to the null ensemble (4), leading to

$$P_\sigma(G) / P_0(G) = Z_\sigma^{-1} \exp[\sigma L(\mathbf{c})] \ . \quad (5)$$

Again the probability $P_\sigma(G)$ that a given subset of nodes $\{r_1, \ldots, r_n\}$ forms a subgraph G depends on the matrix $\mathbf{c}(G)$. We have introduced the normalization factor $Z_\sigma = \prod_{ij} \sum_{c_{ij}=0,1} \exp[\sigma L(\mathbf{c})] \, P_0(G)$, which ensures that $P_\sigma(G)$ summed over all matrices $\mathbf{c}$ gives unity. The quantity σ, called the *link reward*, is multiplied by the total number L of internal links given by (1). The ensemble (5) is a statistically unbiased way to describe that functional motifs are distinguished by a large number of internal links. (Technically, it is the ensemble of maximal information entropy with a given average link number $\langle L \rangle$, which is determined by the value of σ.) This ensemble may be thought of as resulting from an evolutionary process favoring the formation of links due to selection pressure; such a process has recently been studied for regulatory networks [20]. Here we focus on the detection of evolved motifs rather than on the reconstruction of evolutionary histories. Hence, we do not need to make assumptions on dynamical details of motif formation but only on its outcome, which is described by the ensemble $P_\sigma(G)$. We have tested the form of this ensemble for the regulatory network of *E. coli* as discussed in the results section below.

Moreover, the value of the link reward σ can be inferred from the data. One finds $e^\sigma \sim N/n$, which results in a finite expected number $\langle L\rangle/n$ of internal links per node within a motif.

Statistics in the presence of a template

The distribution (5) describes an ensemble with an enhanced number of links, which is appropriate for scoring individual subgraphs in the absence of further knowledge. Consider now an evolutionary process directed towards a given network motif represented by a *template* adjacency matrix $\mathbf{t}$. An alignment $\mathcal{A}$ between the motif $\mathbf{t}$ and the subgraph G is specified by a given ordering of the nodes $\{r_1,\ldots,r_n\}$ in G. The outcome of this evolutionary process can be modeled by an ensemble $Q_{\mathbf{t}}(G,\mathcal{A})$ with a bias against links that do not occur in the template,

$$Q_{\mathbf{t}}(G,\mathcal{A})/P_0(G) = Z_t^{-1}\exp\left[\sigma L(\mathbf{c}) - \frac{\mu}{2}M(\mathbf{c},\mathbf{t})\right]. \tag{6}$$

This denotes the probability that a given subset of nodes $\{r_1,\ldots,r_n\}$ forms an aligned subgraph $(G,\mathcal{A})$, with the definition (3) of the pairwise mismatch of the subgraph G and the template $\mathbf{t}$ in a given alignment $\mathcal{A}$. Again Z_t is given by normalization. This is a *hidden Markov model*: the outcome of the stochastic process is an aligned subgraph $(G,\mathcal{A})$ while only G is observed. The likelihood of observing G is then a sum over all alignments,

$$Q_{\mathbf{t}}(G) = \sum_{\mathcal{A}} Q_{\mathbf{t}}(G,\mathcal{A}). \tag{7}$$

This ensemble has two free parameters, the link reward σ and the mismatch penalty μ (with a factor $1/2$ introduced for later convenience). It is conceptionally similar to hidden Markov models for the alignment of sequences with gaps.

Statistics of correlated subgraphs

Now we turn to the case where a network motif is not given as a template but has to be inferred from a family of suitably aligned subgraphs. The underlying evolutionary process can be regarded as a biased link formation as in the previous section, with the consensus pattern $\overline{c}$ as "template". Assuming the link formation is independent for each subgraph, we obtain an ensemble given by

$$\begin{aligned} Q_{\sigma,\mu}(G^1,\ldots,G^p,\mathcal{A})/\prod_{\alpha=1}^p P_0(G^\alpha) \qquad (8)\\ = Z_{\sigma,\mu}^{-1}\exp\left[\sigma\sum_{\alpha=1}^p L(\mathbf{c}^\alpha) - \frac{\mu}{2}\sum_{\alpha=1}^p M(\mathbf{c}^\alpha,\overline{\mathbf{c}})\right]\\ = Z_{\sigma,\mu}^{-1}\exp\left[\sigma\sum_{\alpha=1}^p L(\mathbf{c}^\alpha) - \frac{\mu}{2p}\sum_{\alpha,\beta=1}^p M(\mathbf{c}^\alpha,\mathbf{c}^\beta)\right], \end{aligned}$$

where $\mathcal{A}$ specifies an alignment of all subgraphs and we have used the definition (2) of the consensus pattern. The normalization is given by

$$\begin{aligned} Z_{\sigma,\mu} \;=\; \sum_{\mathcal{A}}\sum_{\mathbf{c}^1,\ldots,\mathbf{c}^p}\exp\left[\sigma\sum_{\alpha=1}^p L(\mathbf{c}^\alpha)\right. \qquad (9)\\ \left. -\frac{\mu}{2p}\sum_{\alpha,\beta=1}^p M(\mathbf{c}^\alpha,\mathbf{c}^\beta)\right]\prod_{\alpha=1}^p P_0(G^\alpha). \end{aligned}$$

The scoring function

We now construct a *scoring function* designed to select a set of (putatively) functional subgraphs – characterized by a consensus motif with a high number of internal links and low fuzziness – from the background of random subgraphs in a large network.

Based on the preceding discussion, we assume that the statistics of functional motifs is described by an ensemble $Q(G^1,\ldots,G^p,\mathcal{A}) = Q_{\sigma,\mu}(G^1,\ldots,G^p,\mathcal{A})$, where the scoring parameters σ and μ remain to be determined from the data.

For the biological applications described above, where internal links are associated with feedback loops, it is clearly useful to restrict the motif search to the set of all connected subgraphs which contain internal loops, i.e., which are non-treelike. For connected subgraphs of size n, this set is given by the constraint $L \geq n$ on the internal link number. A large random graph typically contains a number of order one of such subgraphs, and these define the relevant null ensemble for motif search. We model these subgraphs using the ensemble P_{σ_0} with an enhanced number of links defined in (5). The parameter σ_0 will be adjusted such that the average number of internal links in the null ensemble equals that found in the non-treelike subgraphs of a suitable randomized graph. Comparing with the ensemble P_0 of random subgraphs introduced earlier, it is clear that the constraint $L \geq n$ corresponds to a link reward $\sigma_0 > 0$.

Given these two ensembles, we define the log-likelihood score

$$\begin{aligned} S(G^1,\ldots,G^p,\mathcal{A}) &= \log\left(\frac{Q_{\sigma,\mu}(G^1,\ldots,G^p,\mathcal{A})}{P_{\sigma_0}(G^1,\ldots,G^p,\mathcal{A})}\right) \\ &= (\sigma-\sigma_0)\sum_{\alpha=1}^{p} L(\mathbf{c}^\alpha) - \frac{\mu}{2p}\sum_{\alpha,\beta=1}^{p} M(\mathbf{c}^\alpha,\mathbf{c}^\beta) \\ &\quad - \log(Z_{\sigma,\mu}/Z_{\sigma_0})\ , \end{aligned} \tag{10}$$

which is positive if a set of subgraphs $G^1,\ldots,G^p$ and an alignment $\mathcal{A}$ between them is more likely to occur in the ensemble $Q_{\sigma,\mu}$ than in the null ensemble P_{σ_0}. The term $\log(Z_{\sigma,\mu}/Z_{\sigma_0})$ acts as a threshold assigning a negative score to alignments with too large fuzziness or a too small number of internal links.

As is clear from the form of the scoring function, graph alignment is a nontrivial optimization problem, the statistical weight of each subgraph G^α depending on the scoring parameters as well as on the other subgraphs included in the alignment. We address this problem in two steps. First we find the maximum-score alignment(s) for given score parameters, which is essentially an algorithmic search problem. Then we discuss the parameter dependence of high-scoring alignments and obtain the optimal values of σ and μ for a given data set from a maximum-likelihood procedure.

Maximum score alignments and parametric optimization

Finding the maximum score alignments involves a huge search space of possible alignments. The number of alignments is of order $(np)^N$ for given p and the computational expense grows further when the optimization over p is performed. Here we use a heuristic algorithm, which can be described by a mapping to a discrete spin model. First we enumerate all non-treelike subgraphs of n nodes, which is feasible for modest values of n, and label them by the index $\alpha = 1,\ldots,p_{\max}$. Next we evaluate the internal link numbers $L^\alpha = L(\mathbf{c}^\alpha)$ and the pairwise mismatches $M^{\alpha\beta}$, defined as the minimum of $M(\mathbf{c}^\alpha,\mathbf{c}^\beta)$ over all *pairwise* alignments of the subgraphs G^α and G^β. High-scoring *multiple* alignments are then found by a simulated annealing algorithm in the space $(s^1,\ldots,s^{p_{\max}})$, where each "spin" s^α takes the value 1 if G^α is included in the alignment and 0 otherwise. The resulting Hamiltonian $\mathcal{H}$ is

$$\begin{aligned} -\mathcal{H} &= (\sigma-\sigma_0)\sum_{\alpha=1}^{p_{\max}} L^\alpha s^\alpha \\ &\quad -\frac{\mu}{2p}\sum_{\alpha,\beta=1}^{p_{\max}} \tilde{M}^{\alpha\beta}s^\alpha s^\beta - \log(Z_{\sigma,\mu}/Z_{\sigma_0})\ , \end{aligned} \tag{11}$$

where $p=\sum_\alpha s^\alpha$. The coupling between s^α and s^β is given by $\tilde{M}^{\alpha\beta}$, which is equal to the pairwise mismatch $M^{\alpha\beta}$ if subgraphs α and β do not overlap, and a large positive constant if they do. (Two subgraphs overlap if they have more than one node in common. According to this definition, links in non-overlapping subgraphs form independently as assumed in (8).) The threshold term $\log(Z_{\sigma,\mu}/Z_{\sigma_0})$ is evaluated by saddle-point integration, details are given in the supporting text. Simulated annealing using the Hamiltonian (11) will then yield high-scoring alignments of non-overlapping subgraphs [22].

For fixed values of the scoring parameters, the algorithm is expected to produce well-defined maximum-score alignments. This can be understood as follows. For a (hypothetical) alignment of subgraphs with equal number of internal links and equal pairwise mismatches, the score (10) scales linearly with p, the number of aligned subgraphs. This is consistent with the interpretation of (10) as a log-likelihood score, since the aligned subgraphs occur independently. A high-scoring alignment in a realistic network may consist of a limited number of identical or very similar motifs. As we extend this alignment to include more subgraphs, subgraphs with increasing mutual mismatches are included. Hence, we expect the total mismatch to increase faster than linearly with p, leading to a maximum $S^*(\sigma,\mu)$ of the total score at some intermediate value of $p^*(\sigma,\mu)$.

The properties of the maximum-score alignments depend strongly on the parameters σ and μ. With increasing σ, the number of internal links $L^*(\sigma,\mu)$ per subgraph is expected to increase. With increasing μ, both the number of graphs $p^*(\sigma,\mu)$ and the fuzziness $\overline{M}^*(\sigma,\mu)$ decrease. In this way, the maximum-score alignment varies between a set of independent subgraphs for $\mu = 0$ and a set of identical subgraphs with identical motifs for $\mu\to\infty$.

A maximum-likelihood approach can be used to infer the optimal scoring parameters σ^*,μ^* for a given data set, which we obtain as the point of the global score maximum $S^* = \max_{\sigma,\mu} S^*(\sigma,\mu)$.

Results and Discussion

In this section, we discuss the application of local graph alignment to motif search in the gene regulatory network of *E. coli*, taken from http://www.weizmann.ac.il/mcb/UriAlon/Network_motifs_in_coli/ColiNet-1.1/, containing 424 nodes and 577 directed links. Each labeled node in this network represents a gene. A directed link between two nodes signifies that the product of the gene represented by the first node acts as a transcription factor on the gene represented by the second. Throughout we consider motifs with a fixed number of nodes $n = 5$.

First we show that our algorithm indeed produces well-defined alignments of maximal score (i.e., of maximal relative likelihood). For fixed parameters $\sigma = 3.8$ and $\mu = 4.0$, this is illustrated by Fig. 2 (a), which shows the score S and the fuzziness $\overline{M}$ for the highest-scoring alignment with a prescribed number p of subgraphs, plotted against p. As expected, the fuzziness increases with increasing p, and the total score reaches its global maximum $S^*(\sigma, \mu)$ at an intermediate value $p^*(\sigma, \mu)$. It is lower for $p < p^*(\sigma, \mu)$ since the alignment contains less subgraphs and for $p > p^*(\sigma, \mu)$ since the subgraphs have higher mutual mismatches. Fig. 2 (b) shows the score $S^*(\sigma, \mu)$ as a function of σ and μ. This function has a unique global maximum S^*, which defines the maximum-likelihood point $(\sigma^* = 3.8, \mu^* = 2.25, p^* = 24)$.

The scoring parameter σ_0 of the null ensemble P_{σ_0} is determined as follows: the data set is randomized by generating a network with the same connectivities as in the data set but randomly chosen links [18, 10]. Again, the non-treelike subgraphs are extracted and their average number of internal links is determined. The value of σ_0 is uniquely determined by the condition that the expected number of links in the null ensemble (5) equals the average number of internal links found in the non-treelike subgraphs. One obtains $\sigma_0 = 2.45$. As expected, $\sigma_0 < \sigma^*$, which shows that the data set has an enhanced number of internal links relative to the randomized network.

At the maximum-likelihood scoring parameters, we can moreover verify the functional form of the ensembles used to construct the score function (10). In order to test the model (5) for individual subgraphs, we enumerate all subgraphs with $n = 5$ that have non-treelike patterns (i.e., a link number $L \geq 5$). All ordered pairs of nodes i, j are then binned according to the the probability w_{ij} of a directed link existing between them in the ensemble $P_0(G)$. In Fig. 3 (a) the fraction of these pairs i, j carrying a link is plotted against w (square symbols). The expectation value of this fraction is given by (5) as $\mathrm{e}^\sigma w/(1 - w + \mathrm{e}^\sigma w)$, shown as a solid line with a fit value $\sigma^* = 3.8$.

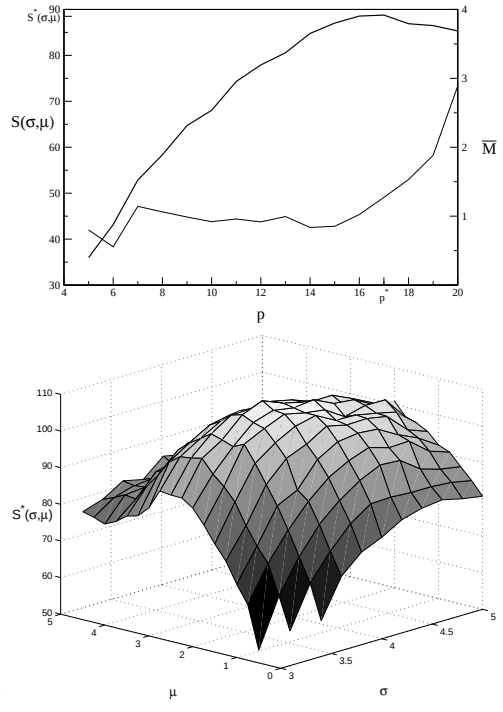


Figure 2: **Maximum score alignment and parametric optimization**. (a) Score optimization at fixed scoring parameters $\sigma = 3.8$ and $\mu = 4.0$. The total score S (thick line) and the fuzziness $\overline{M}$ (thin line) are shown for the highest-scoring alignment of p subgraphs, plotted as a function of p. (b) The score $S^*(\sigma, \mu)$ plotted against the parameters μ and σ. The unique maximum S^* defines the maximum-likelihood parameters $\sigma^* = 3.8$ and $\mu^* = 2.25$.

Our model (8) for generic alignments can be tested in a similar way. From this ensemble, the marginal probability that a given ordered pair of nodes specified by α, i, j is linked can be computed. We group all such pairs with the same expectation value $\langle c_{ij}^\alpha \rangle_{\sigma^*, \mu^*}$ according to (8) to build a histogram. For each group, the average of c_{ij}^α over node pairs in the actual maximum-likelihood alignment is computed and plotted against the model prediction, see fig. 3(b). The same procedure is repeated for the two-point correlations $\langle c_{ij}^\alpha c_{ij}^\beta \rangle_{\sigma^*, \mu^*}$ between associated nodes in different subgraphs α and β as also shown in fig. 3(b). In both histograms, the data points cluster well around the straight line equating expectation values in the model (8) and averages in the actual alignment. The fluctuations seen reflect the limited size of the data set and the small number of fitting parameters in

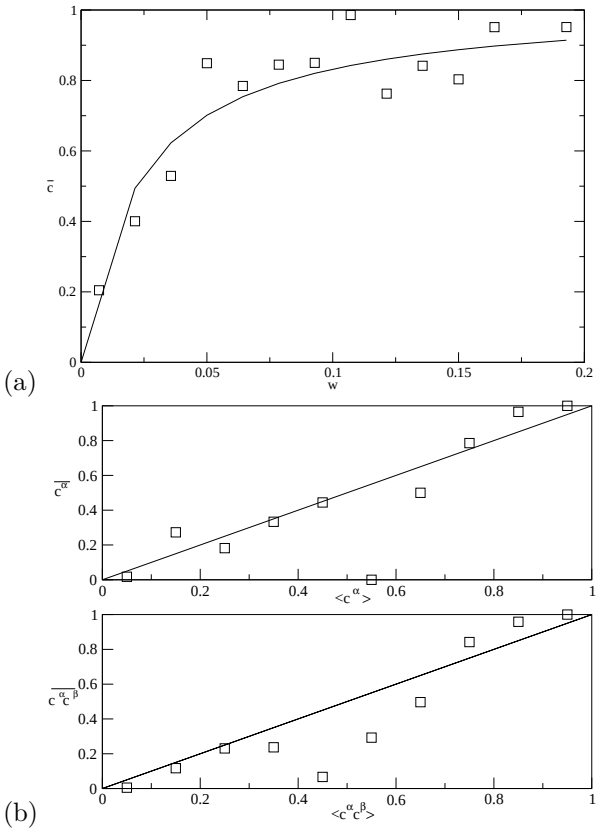


Figure 3: **Statistics of motif ensembles.** (a) Testing the statistical model for single subgraphs (5). Non-treelike subgraph are enumerated and node pairs i, j binned according to w_{ij}. The fraction of such pairs carrying a link is shown against w_{ij}. The solid line results from fitting the model with enhanced number of links (5) to this data, giving $\sigma = 3.8$. (b) Testing the statistical model for alignments (8). Top: The average value of c_{ij}^{α} over all α, i, j with a given expectation value of c_{ij}^{α} according to (8) at $\sigma = \sigma^* = 3.8$ and $\mu = \mu^* = 2.25$ against the corresponding expectation value (squares). For a perfect fit between model and data a straight line is expected (shown solid). Bottom: The same procedure is used averaging the two-point function $c_{ij}^{\alpha} c_{ij}^{\beta}$ over all α, β, i, j with a given expectation value $\langle c_{ij}^{\alpha} c_{ij}^{\beta} \rangle$.

the model. For such data, more detailed models can hardly be tested since they would lead to overfitting.

We now turn to the probabilistic consensus motifs found in the data for different number of nodes $n = 4$ and $n = 5$. Fig. 4(a) shows the $n = 4$ consensus motif $\bar{c}_{ij}$ at consecutive values of $\mu = \mu^* = 3.6$, $\mu = 8$, and $\mu = 15$. The gray-scale encodes the average number of links $\overline{c}_{ij}$ between a given pair of nodes. As expected, the fuzziness decreases with increasing values of the mismatch penalty μ and $\overline{c}_{ij}$ tends either to zero (no link present) or one (link present with certainty) as $\mu \to \infty$. The consensus motif is a layered structure, in this case with 2 input and 2 output nodes.

A similar motif is found for $n = 5$. Fig. 4(b) shows the $n = 5$ consensus motif at consecutive values of $\mu = 2.25, 5$, and 12. As in the case of $n = 4$, a layered structure is clearly discernible: the motif consists of $2 + 3$ nodes forming an input and an output layer, with links largely going from the input to the output layer. The left node of the input layer has an average number of about 30 outgoing links. These connectivities are exceptional since the average out-connectivity of the network is 1.36.

Comparing the alignments of subgraphs of $n = 4$ nodes with those of $n = 5$ nodes in figure 4, one finds that many of the subgraphs found in the $n = 4$-alignments also are a part of the subgraphs found in the $n = 5$-alignments. This immediately leads to the question of how to identify *larger* patterns in the network from which the subgraphs at a given value of n are taken. Obviously any scoring scheme operating at a fixed number of nodes n will be blind to the combinatorial possibilities of selecting subgraphs from a larger pattern. The phenomenon is exemplified in figure 4(c). From the 3-by-4 pattern 2 non-overlapping layered subgraphs with $n = 4$ and $n = 5$ can be generated (non-overlapping subgraphs have at most one node in common, see above). Larger patterns generate correspondingly more non-overlapping subgraphs. In the supporting text, we discuss a simple scheme which allows to identify larger patterns as in figure 4(c) from smaller subgraphs. The pattern of figure 4(c) is found twice in the data, contributing in total 4 non-overlapping subgraphs to the alignments with $n = 4$ and $n = 5$. The statistics of these patterns at the level of *identical patterns* has recently been analyzed in [23], their treatment using *probabilistic patterns* remains a future development.

Figure 4(d) shows details of the alignments producing the consensus motifs at $n = 5$, namely, the number of subgraphs $p^*(\sigma = \sigma^*, \mu)$ and the fuzziness $\overline{M}^*(\sigma = \sigma^*, \mu)$ plotted as a function of μ. For $\mu > 12$ the fuzziness reaches zero and the alignment contains 10 identical, non-overlapping motifs. This layered pattern has been found by the approach of ref. [6], which is based on counting identical motifs. However, the maximum-likelihood alignment occurs at $\mu^* = 2.25$ and contains a much larger number of $p^* = 24$ non-overlapping subgraphs, leading to the probabilistic consensus motif shown on the left in fig. 4(a). The same effect is found in the consensus-motif of size $n = 4$. Furthermore, at arbitrary non-

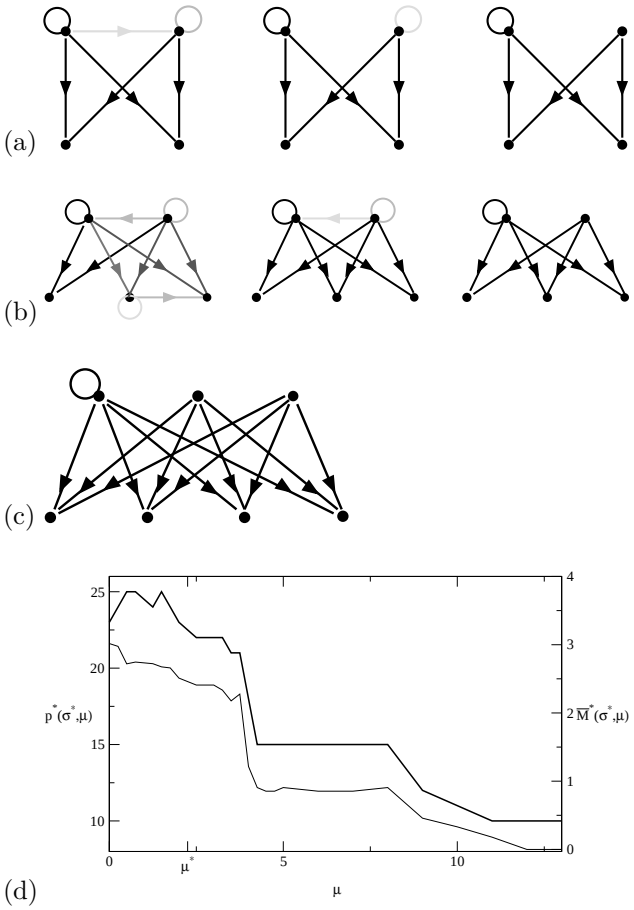


Figure 4: **Probabilistic motifs in the E. coli transcription network.** (a) Consensus motifs with $n = 4$ nodes at different values of μ. From left to right, $\mu = \mu^* = 3.6$, $\mu = 8$, and $\mu = 15$. The gray-scale of the links indicates the likelihood that a given link is present in the aligned subgraphs; the 5 gray values correspond to $\bar{c}$ in the range $0.1 - 0.2$, $0.2 - 0.4$, $0.4 - 0.6$, $0.6 - 0.8$, $0.8 - 0.9$, links with $\bar{c} > 0.9$ are shown black. The link reward is kept fixed at $\sigma = \sigma^* = 3.6$ and σ_0 takes on the value 3.15. (b) Consensus motifs with $n = 5$ for different $\mu = \mu^* = 2.25$, $\mu = 5$, and $\mu = 12$ (left to right) at $\sigma = \sigma^* = 3.8$. (c) This pattern with $n = 7$ is found twice in the data-set. From each such subgraph 2 non-overlapping layered subgraphs with $n = 4$ and $n = 5$ can be generated. (d) The number $p^*(\sigma^*, \mu)$ of subgraphs in the maximum score alignment (thick line) and the fuzziness $\overline{M}^*(\sigma^*, \mu)$ (thin line) as a function of μ for $n = 5$.

zero fuzziness the probability that a given pair of subgraphs have *identical motifs* decreases with subgraph size. As a result, counting identical motifs, rather than following a probabilistic approach as the one presented here, will miss an fraction of relevant subgraphs present in the data which increases with the size of the subgraph.

The probabilistic grounding of motif search is also indispensable for quantitative significance estimates of the results obtained. Here we compare the maximum-likelihood alignment in the *E. coli* data set with suitable random graph ensembles. We do this in two steps, in order to disentangle the significance of the number of internal links, and of the mutual similarity of patterns found in the data.

(i) To assess the significance of the number of internal links, we consider the ensemble of graphs with the same in- and out-connectivities as the data set but randomly chosen neighbors [18, 10] and compute the distribution of the score with scoring parameters $\sigma = \sigma^*$, $\mu = 0$. The null distribution of scores from the randomized graph has the average and standard deviation given by $S^* = 5.7 \pm 2.1$. The score $S^* = 73.1$ found from the data is thus significantly higher, indicating an enhanced link number with respect to the random graph ensemble. (ii) The significance of the mutual similarity of the aligned patterns is assessed by comparing the data to mutually independent random subgraphs with the same average density of links. (This null ensemble is generated by randomizing the internal links of each subgraph independently.) We then compute the score with parameters $\sigma = \sigma_0 = \sigma^*$ and $\mu = \mu^*$ (thereby only focusing on the fuzziness of the data relative to that found in the ensemble of uncorrelated subgraphs). This null distribution of scores has average and standard deviation given by $S^* = 27.1 \pm 6.3$; the corresponding score $S^* = 50.1$ found from the data is thus significantly higher. We note that the assessment of subgraph similarity is quite subtle. Subgraphs taken from a large but finite random graph may show a 'spurious' mutual similarity with respect to independent random subgraphs due to a prevalence of internal loops.

The statistical significance of the results can be formulated more precisely using so-called p-values, which involve the tail of the score distribution in the random graph ensemble. Fast and reliable p-value estimates are crucial for the search in large databases, as it is well known for sequence alignment [21]. This approach can be carried over to the graph alignments discussed here.

The statistical framework presented is very flexible. For example, as large-scale data on the logic of gene regulation become available, the definition of the pairwise mismatch (3) can be extended to reward aligning sets of nodes performing the same logical function. In this way, features of motifs going beyond their topology can be explored. Similarly, simple modifications of the mismatch score al-

low the analysis of undirected networks, networks whose links have a specific function (repressive or enhancing) or whose interaction strength is quantified by a real number. The statistical framework presented is very flexible. For example, as large-scale data on the logic of gene regulation become available, the definition of the pairwise mismatch (3) can be extended to reward aligning sets of nodes performing the same logical function. In this way, features of motifs going beyond their topology can be explored. Similarly, simple modifications of the mismatch score allow the analysis of undirected networks, networks whose links have a specific function (repressive or enhancing) or whose interaction strength is quantified by a real number.

The prospect of a sizable amount of new data on biological networks becoming available over the next few years through high-throughput methods opens exciting opportunities to identify the building blocks of molecular information processing in a wide range of organisms, and even build phylogenetic histories of regulation from transcription network data.

Acknowledgments: Many thanks to T. Hwa for fruitful discussions and to U. Alon and P. Arndt for comments on the manuscript. This work has been supported through DFG grant LA 1337/1-1. We thank the KITP Santa Barbara, ICTP Trieste, the Centro di Ricerca Matematica Ennio De Giorgi, Pisa, and the Aspen Center for Physics for hospitality during various stages of this work.

References

[1] Durbin,R., Eddy,S.R., Krogh,A., & Mitchison,G. (1998) *Biological sequence analysis*, (CUP, Cambridge, UK).

[2] Davidson,E.H. (2001) *Genomic regulatory systems: Development and Evolution* (Academic Press).

[3] Tautz, D. (2000) *Current Opinion in Genetics & Development* **1**, 575-579.

[4] Uetz,P., Giot,L., Cagney,G., Mansfield,T. A., Judson,R. S., Knight J.R., Lockshon D., Narayan V., Srinivasan M., Pochart P., Qureshi-Emili A., Li Y. et al.(2000) *Nature* **403**, 623-627.

[5] Lockhart,D.J., & Winzeler,E.A. (2000) *Nature* **405**,827-836.

[6] Shen -Orr,S., Milo,R., Mangan,S., & Alon,U. (2002) *Nature Genetics* **31** 64-68.

[7] Milo,R., Shen-Orr,S., Itzkovitz,S., Kashtan,N., Chklovskii,D. & Alon,U. (2002) *Science*, **298** 824-827.

[8] Newman,M.E.J., Strogatz,S.H., & Watts,D.J. (2001) *Phys. Rev.* **E 64**, 026118.

[9] Newman,M. (2002) *Phys. Rev. Lett.* **89**, 208701.

[10] Berg,J., & Lässig,M. (2002) *Phys. Rev. Lett.* **89**, 228701.

[11] Costas,J., Casares,F., & Viera,J. (2003) *Gene* **310** 215-220.

[12] Stormo,G.D., & Hartzell,G.W. (1989) *Proc. Nat. Acad. Sci. USA* **86**, 1183-1187.

[13] Bussemaker,H.J., Li,H., & Siggia,E.D. (2000) *Proc. Nat. Acad. Sci. USA* **97**, 10096-10100.

[14] Felsenstein,J. (1981) *Journal of Molecular Evolution* **17** 368-376.

[15] Ullmann,J.R. (1976) *Journal of the Association for Computing Machinery* **23** 31-42.

[16] Messmer,B.T.,& Bunke,H. (1998) *IEEE Trans. on Pattern Analysis and Machine Intelligence* **20 (5)** 493-504.

[17] Garey,M.R. & Johnson,D.S. (1979) *Computers and Intractability: A Guide to the Theory of Np-Completeness* (Freeman,NY).

[18] Maslov,S., & Sneppen,K. (2002) *Science* **296** 910-913.

[19] Itzkovitz,S., Milo,R., Kashtan,N., Ziv,G., & Alon,U. (2003) Phys. Rev.**E 68**, 026127.

[20] Berg, J., Lässig,M., & Radic,S. (2003) http://arxiv.org/abs/cond-mat/0301574 .

[21] Karlin,S., & Altschul,S.F (1990) *Proc. Nat. Acad. Sci. USA* **87** 2264-2268.

[22] Blat,M., Wiseman,S., & Domany,E. (1996) *Phys. Rev. Letters* **76** 3251-3255.

[23] Kashtan,N., Itzkovitz,S., Milo,R., & Alon,U. (2003), http://arXiv.org/abs/q-bio/0312019

Supporting Text

In the supplementary material we first give additional details on the alignment algorithm and then discuss a simple procedure for identifying larger modules generating multiple smaller subgraphs.

The algorithm proceeds in four stages:

1. By enumeration all unique non-treelike subgraphs of size n are found. We consider only subgraphs where each node carries at least two internal links, other than self-links ("exclusion of dangling links"). The reason is that including dangling links would generate from each subgraph an artificially inflated family of subgraphs generated by including all combinations of neighboring nodes into the subgraph. The enumeration is done by first finding all closed paths in the graph of length shorter than $2n-3$. (The maximum length derives from considering the non-treelike structure with the longest pathlength from the origin through all points of the subgraph back to the origin. The graph is considered as undirected at this stage.) The subgraphs are labeled by $\alpha = 1, \ldots, p^{\max}$.

2. The pairwise minimal mismatch $M^{\alpha\beta}$ for all *pairs of subgraphs* α, β is found by enumerating all $n!$ possible alignments of each pair of subgraphs. For each pair of subgraphs α and β we determine whether they overlap by counting the number of nodes they have in common. The elements of the coupling matrix $\tilde{M}^{\alpha\beta}$ in the Hamiltonian **11** are given by $M^{\alpha\beta}$ if the subgraphs do not overlap, and by a large number, chosen to be 10, if they do.

3. The next task is to select a subset of the subgraphs such that the total score **10** is maximized at given values of the scoring parameters. To this end simulated annealing is used, with the (negative) score as the energy function, increasing the inverse temperature from 0 to 10 in 1000 Monte-Carlo sweeps. We assign each *subgraph* a spin variable: spin $s^\alpha = 1$ implies that the subgraph α is included in the alignment, spin $s^\alpha = 0$ that it is not. The contribution to Eq. **10** from the mismatch of two subgraphs acts as a coupling between their spins, the contribution of subgraph α to the total number of links L in **10** acts as a local field, resulting in the Hamiltonian **11**. The evaluation of the last term in **10**, $\log(Z/Z_0)$, is discussed below.

The last step is repeated at different values of σ and μ in order to perform the parametric optimization leading to Fig. 2*b*. The parameter σ_0 describing the null ensemble, on the other hand, is determined independently by considering the non-treelike subgraphs found in the randomized graph as described in the paper. σ_0 is chosen such that the average number of internal links in the ensemble of uncorrelated subgraphs with an enhanced number of links **5** equals that of the non-treelike subgraphs found in the randomized network,

$$\frac{1}{p}\sum_{\alpha=1}^{p}\langle L(\mathbf{c}^\alpha)\rangle_{\sigma_0,\mu=0} = \overline{L}_{\text{randomized}} \ .$$

Note that the ensemble **5** still depends on the connectivities of the nodes in each subgraph. The generalization to several *groups of subgraphs*, where only subgraphs from the same group are aligned with each other, can be done by admitting more states of the Potts-like spins s^α. For q-state spins this would group the subgraphs into $q-1$ clusters much like in superparamagnetic clustering (1).

There are two approximations behind this algorithm. First, treelike subgraphs are excluded from the start. This step cuts down an enormous number of combinatorial possibilities associated with treelike subgraphs, which, different connectivities apart, are always locally similar.

Second, it uses the minimal mismatch obtained from the *pairwise* alignment of subgraphs (step 2), even though the minimal mismatch obtained by aligning a set of more than two subgraphs may be higher than that of the sum of pairwise alignments. This is easily seen by comparing the total number of alignments of all *pairs* chosen from p subgraphs, $(n!)^{p(p-1)/2}$, with the number of alignments of p subgraphs, $(n!)^p$. However, in the case of interest, where the graph contains multiple copies of a motif (possibly corrupted by noise), the sum of pairwise minimal mismatches will typically be very close to the minimal mismatch obtained from aligning all subgraphs simultaneously.

The maximal-score alignment $\mathcal{A}^\star(\sigma,\mu)$ turns out to be unique in most subgraphs. To see this, consider all alignments $\mathcal{A}^\alpha$ of a particular subgraph α with respect to the other subgraphs whose alignment is kept fixed. Two different alignments have the same score if and only if there is a permutation of the nodes $r_1^\alpha, \ldots, r_n^\alpha$ leaving both the adjacency matrix c_{ij}^α and the matrix w_{ij}^α defined above Eq. **4** invariant. While symmetries of the adjacency matrices occur frequently, entries of the matrix w_{ij} are unique in most subgraphs, since the connectivities in biological

networks are broadly distributed.

We now discuss the normalizing constant **9** of the alignment ensemble **8**. We approximate the likelihood of given parameter values, which involves the sum over all alignments $\mathcal{A}$ as in **9**, by the corresponding maximum-score alignment. (In the literature for sequence alignment, this is known as the Viterbi approximation.) An improved likelihood estimate is possible using probabilistic graph alignment algorithms but is not expected to alter our results qualitatively. The optimal alignment has $p^\star \equiv p^\star(\sigma^\star, \mu^\star)$ subgraphs with average internal link number $\overline{L}^\star \equiv \overline{L}^\star(\sigma^\star, \mu^\star)$ and fuzziness $\overline{M}^\star \equiv \overline{M}^\star(\sigma^\star, \mu^\star)$. As may be seen by differentiation of **10** with respect to the scoring parameters, at $\sigma = \sigma^\star$ and $\mu = \mu^\star$ the Q ensemble fits to the data set in the sense that the expectation values of the internal link number and the fuzziness equal the actual values,

$$\frac{1}{p}\sum_{\alpha=1}^{p}\langle L(\mathbf{c}^\alpha)\rangle_{\sigma^\star,\mu^\star} = \overline{L}^\star,$$

$$\frac{1}{p^2}\sum_{\alpha,\beta=1}^{p}\langle M(\mathbf{c}^\alpha,\mathbf{c}^\beta)\rangle_{\sigma^\star,\mu^\star} = \overline{M}^\star.$$

The normalizing constant **9** needs to be computed for two sets of parameters; for σ, μ characterizing the Q ensemble, and for σ_0, μ_0 characterizing the Q_0 ensemble. In both cases the normalizing constant consists of a trace over the link configuration $\{\mathbf{c}^\alpha\}$ in all subgraphs. Since the constant **9** factorizes in the link labels i, j, we consider only a single of these factors (a single "string"), drop the i, j indices, and separate the bilinear form of the pairwise mismatch **3** into a quadratic and a linear part.

Formally, this expression is the partition function of a mean-field ferromagnet in a fluctuating field. The field depends on the local connectivities of each node along the "string" via the ensemble P_0, Eq. **4**. Using a Hubbard-Stratonovich transformation to linearize the quadratic term, the trace over $\{c^\alpha\}$ can be performed, giving

$$Z = \int \frac{dt}{\sqrt{2\pi/p}} \exp\left\{-pt^2/2 + \sum_{\alpha}^{p} g^\alpha(t)\right\} \ , [\mathbf{12}]$$

where

$$g^\alpha(t) = \log\left[(1-w^\alpha) + w^\alpha \exp\left\{\sqrt{2\mu}t + \sigma - \mu\right\}\right] \ .$$

For large p this expression can be evaluated by a saddle point integral, giving

$$\log Z \approx -pt^{\star 2}/2 + \sum_{\alpha}^{p} g^\alpha(t^\star) + \mathcal{O}(\log p) \ ,$$

where $t^\star$ maximizes the exponent in Eq.**12**. The contribution to leading order of adding a new subgraph with index α is thus

$$\Delta \log Z \approx -t^{\star 2}/2 + g^\alpha(t^\star) \ .$$

The change of $t^\star$ as a finite number of subgraphs is added to or removed from the alignment alters the result only by terms of order p^{-1}. It thus turns out to be sufficient to update the saddle-point value $t^\star$ for each link i, j once per Monte-Carlo sweep of the algorithm.

In order to compute for each pair i, j in the Viterbi approximation, the one-to-one mapping between nodes in each subgraph $\mathcal{A}$ is needed, going beyond the *pairwise* alignment. This mapping is also needed to produce the plots of the consensus motifs in Fig. 4. It is produced by minimizing the fuzziness over the mapping between nodes in each subgraph, again using Monte-Carlo dynamics (100 Monte-Carlo sweeps while linearly increasing the inverse temperature from 0 to 10). The result of course depends on the subgraphs in the alignment, and thus the mapping ought to be updated each time a subgraph is added or removed from the alignment. In practice, however, one update of the mapping between nodes in each subgraph every 250 steps of the algorithm is sufficient. The reason for this is again that the mapping between nodes in subgraphs in the alignment is unchanged as motifs sufficiently close to the consensus motif enter/leave the alignment.

Finally, we discuss a simple procedure for identifying these structures *from the set of subgraphs at fixed (small) n*. First, for a given subgraph of size n, all neighbors with at least two links to the subgraph are enumerated. In this way, non-treelike subgraphs without dangling bonds with $n+1$ nodes are generated. This procedure is repeated for the entire list of p subgraphs. Several subgraphs of size $n+1$ will occur repeatedly in this list: the more subgraphs of size n can be be generated from the larger $n+1$ subgraph the more frequently it occurs on the list. Thus ranking the $n+1$ subgraphs according to the number of times they occur in the list, one obtains the $n+1$ subgraph from which the largest number of n subgraphs derive. Clearly this procedure can be repeated iteratively, leading to subgraphs of increasing size. In fact, Fig. 4 *c* is the result of applying this scheme to the non-treelike subgraphs with $n = 5$. Iterating twice, one finds two instances of the $n = 7$ layered structure of Fig. 4*c*.

[1] Blat,M., Wiseman,S., & Domany,E. (1996) *Phys. Rev. Lett.* **76** 3251-3255.